University of Glasgow

DEPARTMENT OF

AEROSPACE ENGINEERING

Chicago Beach Resort Development – A Review of Galloping of Rectangular Prisms Pertinent to the Stability of the Tower Hotel External Frame.

by

M. Vezza

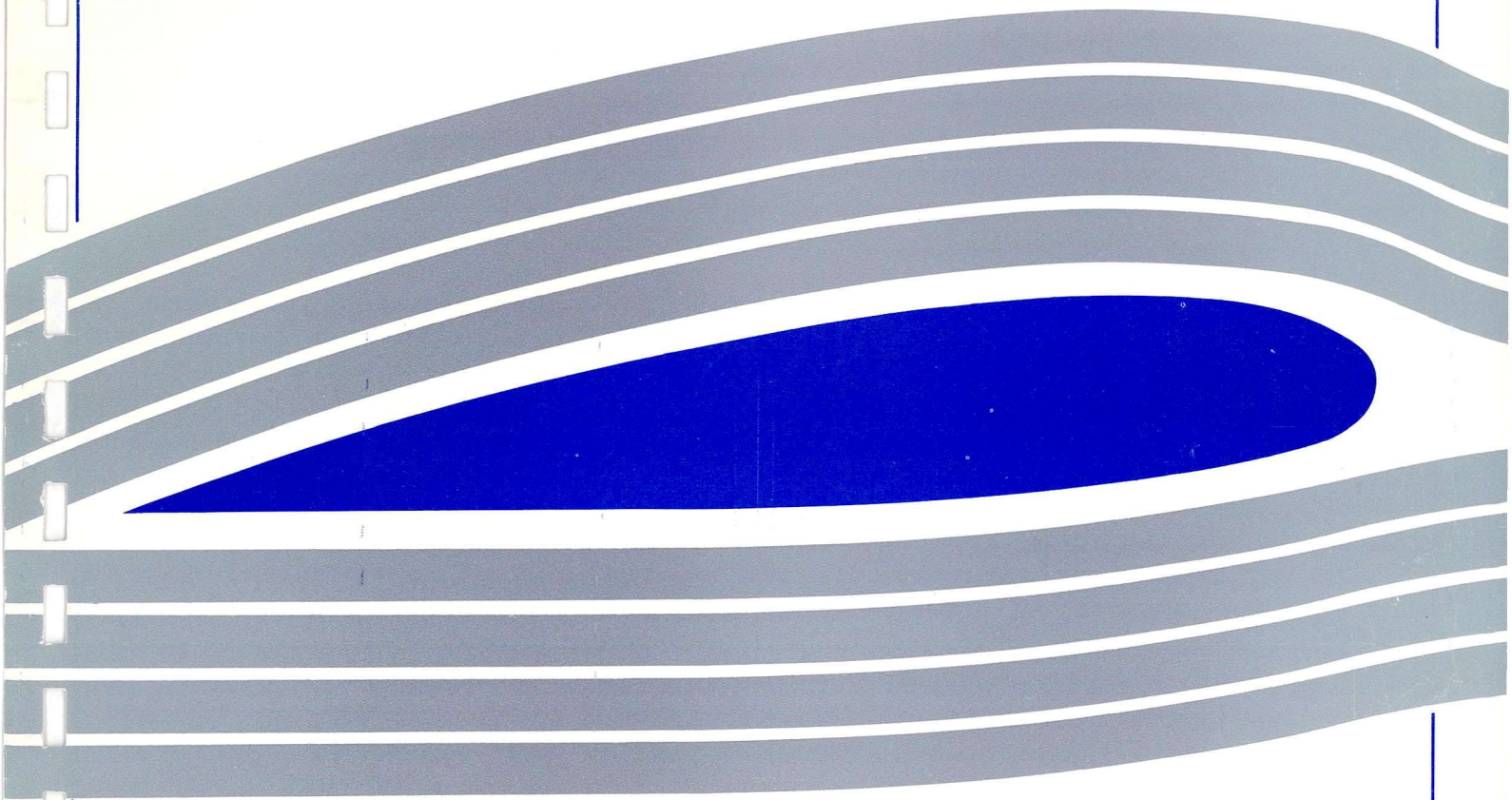

UNIVERSITY
of
GLASGOW

Chicago Beach Resort Development – A Review of Galloping of Rectangular Prisms Pertinent to the Stability of the Tower Hotel External Frame.

by

M. Vezza

Department of Aerospace Engineering
University of Glasgow
Glasgow G12 8QQ.

on behalf of

W.S. Atkins and Partners Overseas.

G.U. Aero Report No. 9619
September 1996.

SUMMARY.

In this report a review, commissioned by W.S. Atkins and Partners Overseas, is presented of the factors which determine the high speed galloping stability characteristics of rectangular prisms. The information is subsequently used to make an assessment of the galloping stability of the external frame of the Tower Hotel, a structure which forms part of the Chicago Beach Resort Development. The predictions of linear theory are explained, and the effects of aspect ratio, freestream turbulence and reduced damping discussed in detail. The variety of oscillatory response is explained with reference to both non-linear theory and results from wind tunnel experiments. A number of prevention methods are proposed, based on results from model and full-scale tests. It is concluded that the factors discussed can have a marked effect on the galloping tendency and response of rectangular prisms.

Notwithstanding the limitations of the sectional aerodynamic theory employed, an assessment of the transverse galloping stability of the Tower Hotel external frame is made. The added dampers, originally designed to suppress vortex excitation, also play an important role in the suppression of galloping in the upper two bays of the exoskeleton. With these dampers the calculated threshold wind speeds are substantially in excess of those likely to occur in the top two bays, even in extreme conditions. Without the dampers galloping excitation would be possible, especially in low turbulence flows. The lower two bays have higher natural frequencies and mass, and experience lower wind speeds. The corresponding level of damping required may be achievable without dampers.

No published data has been found to enable an assessment to be made of the aeroelastic stability of the Tower Hotel mast. Although circular sections do not gallop, very slight deviations from circularity may result in an unstable section. The situation is exacerbated by the lower turbulence intensities at this height, as well as the given slenderness, exposure and fixing arrangements. It is recommended, therefore, that a series of aerodynamic tests be performed to investigate the stability of the mast.

CONTENTS.

1. INTRODUCTION.

W.S. Atkins and Partners Overseas have indicated concern about the aeroelastic stability of the external frame of the Tower Hotel, illustrated in Fig. 1.1, which forms part of the Chicago Beach Resort Development. The external frame of the hotel is composed of prismatic members of rectangular section, additionally supported by lattice frameworks. To address this concern, W.S. Atkins have commissioned a review of the factors which determine the galloping stability of rectangular prisms, pertinent to the structural data of the external frame. The commission followed on from a proposal which was submitted to the consultants for consideration.

The Chicago Beach Resort Development is a planned new tourist resort, located approximately 15km from the centre of Dubai, United Arab Emirates. The development, Fig. 1.2, comprises two hotels: the Tower Hotel, 280m high , located on an artificial island centred 360m from the shore; the onshore Tourist Hotel, approximately 100m high and 275m long.

This report is the result of the requested review, and aims to provide W.S. Atkins with an explanation of the basic mechanism of the phenomenon known as high speed transverse galloping. The main factors affecting transverse galloping, and the oscillatory characteristics of galloping prisms, are discussed in some detail. Notwithstanding the limitations of the underlying theory, calculations are presented which enable an assessment to be made of the galloping stability of the Tower Hotel exoskeleton.

2. GALLOPING OF RECTANGULAR PRISMS.

In this section, a review is presented of the most significant work carried out into the phenomenon of galloping excitation, with particular reference to rectangular prisms. The review begins with a description of the mechanism of galloping, followed by a discussion of the factors and parameters affecting the type of galloping instability which can occur. Some of the studies have investigated possible means of alleviation, and these are also presented.

2.1. Basic Mechanism of Galloping.

The concept of galloping excitation has been around for most of the twentieth century, but the first detailed explanation of the mechanism is generally credited to Den Hartog (1930). Of primary concern is high speed galloping, so called because the reduced velocities associated with this phenomenon are well in excess of those for vortex excitation. Typically a factor greater that four distinguishes the reduced velocity of galloping from vortex excitation (Nakamura, 1990). This means that the assessment of instabilty can be performed using quasi-steady aerodynamic theory, in which the static characteristics of the body corresponding to the instantaneous angle of attack are used (Parkinson and Brooks, 1961). As

illustated in Fig. 2.1, a body which presents an asymmetric profile at non-zero angles of incidence will generate lift and drag forces due to the pressure distribution on the side (and rear) faces.

The equation governing the transverse motion of the prism is given by

$$m\ddot{y}+c_s\dot{y}+k\,y=\frac{1}{2}\rho V^2 h C_y$$

where C_y is the static transverse force coefficient related to the lift and drag coefficients obtained from tests:

$$C_y=-\sec\alpha\left[C_L+C_D\tan\alpha\right]$$

and angle of incidence $\alpha=\tan^{-1}\left(\frac{\dot{y}}{V}\right)$.

At the onset of instability the incidence is small, and the following approximations can be made:

$$\alpha\approx\tan\alpha=\frac{\dot{y}}{V}\quad\text{and}\quad C_y\approx\left.\frac{dC_y}{\mathrm{d}\alpha}\right|_{\alpha=0}\alpha$$

Substituting into the dynamic equation, the nett damping, d, can be written:

$$d\;=\;2mN\delta_s\;-\;\frac{1}{2}\rho V h\left.\frac{dC_y}{d\alpha}\right|_{\alpha=0}$$

where N, δ_s are the natural frequency (Hz) and logarithmic damping for the structure.

The system tends toward oscillatory instability when $d<0$, and this can occur only if

$$\left.\frac{dC_y}{d\alpha}\right|_{\alpha=0}>\;0\qquad\text{or}\qquad\left.\left(\frac{dC_L}{d\alpha}+C_D\right)\right|_{\alpha=0}<\;0$$

A condition for instability, therefore, is that the cross-sectional lift coefficient possesses a negative slope.

The critical velocity above which galloping oscillations are predicted to occur is easily extracted:

$$V_{crit}\;=\;\frac{4mN\delta_s}{\rho h\left.\frac{dC_y}{d\alpha}\right|_{\alpha=0}}$$

The corresponding reduced velocity is simply $V_r=\frac{V}{Nh}$.

It is easily shown that for oscillations about a non-zero mean angle, $\overline{\alpha}$, the transverse force derivative in the above critical speed equation is replaced by $\left.\frac{dC_y}{d\alpha}\right|_{\alpha=\overline{\alpha}}\cos\overline{\alpha}$. The cosine

term is a reducing factor and, as explained in section 2, the transverse force derivative is normally smaller at non-zero incidence. Hence the lowest critical speed is usually estimated for flow at zero incidence.

This assessment, based on linear theory and sectional aerodynamics, suffices in many instances when the aim is to establish the tendency or otherwise for galloping instability to occur. However a full description of the subsequent galloping motion requires a non-linear representation of force coefficient C_y, normally expressed in powers of $\frac{\dot{y}}{V}$, as initially proposed by Parkinson and Brooks (1961). In addition, galloping instability can occur in circumstances not predicted by the linear theory.

2.2. Effect of Aspect Ratio and Freestream Turbulence on Galloping Speed.

As discussed in Parkinson (1974), and later, among others, by Nakamura and Hirata (1993), the aspect ratio (*d/h*) of a rectangular cylinder has a very significant effect on its galloping behaviour. The amplitude $\left(\overline{Y}_s / U\right)_{\max}$ curve in Fig. 2.2, taken from Parkinson (1974), indicates that galloping from rest, that is, pertaining to a *soft oscillator*, occurs over the limited range $0.75 < d/h < 3$.

Investigations by various workers (Bearman and Trueman, 1971; Brooks, 1960; Smith, 1962) have indicated that the structure of the shear layers behind the separation points and their influence on the pressure distribution plays the principal role. As the aspect ratio increases from values below 0.75 the shear layers curve more noticeably inwards towards the body until a *critical depth* is reached, beyond which the slope of the force coefficient rapidly changes sign, Fig. 2.3 (Nakamura, 1993).

Prisms for which $d/h > 3$ are stable with respect to transverse galloping because the shear layers reattach to the sides of the body and produce a transverse force which opposes motion. Galloping is still possible for $d/h < 0.75$, but requires an initial threshold amplitude in smooth flow. Such behaviour identifies a *hard oscillator*, more of which is mentioned below.

The above explanation is, however, affected by the intensity of freestream turbulence, as also indicated in Fig. 2.3. Indeed, turbulence modifies the process of flow reattachment on the sides of the body, the effect of which can be to turn a hard oscillator into a soft one, as illustrated by the sign of the force derivative in Fig. 2.3(b). This interpretation is supported by the results of static experiments on rectangular prisms in turbulent air. Figure 2.4 (Laneville and Parkinson, 1971) illustrates the effect of turbulence on prisms with $d/h = 0.5$ and 2. Fig. 2.4(a) indicates that the oscillator characteristics of the low aspect ratio section become progressively softer with increasing turbulence intensity, and instablity is expected at the highest intensity of 12%. The opposite is true of the high aspect ratio section in Fig. 2.4(b). This section becomes a progressively weaker soft oscillator with increasing turbulence

intensity, and at 12% the section is completely stable. In Fig. 2.4(c), where $\overline{U}_r = \frac{V_r}{2\pi}$, the weakening instability with increasing turbulence of the high aspect ratio section is evident from the decrease in amplitude for a given reduced velocity.

Similar conclusions were drawn by Novak and Tanaka (1974), who investigated the stability of rectangular prisms with d/h = 3/2 and 2/3. They additionally carried out an investigation of the interaction of turbulence with three dimensional effects, by peforming tests on a free standing prism. The results for the 3/2 rectangle are shown in Fig. 2.5. It is notable that the weakening oscillator characteristics of this prism , with increasing turbulence intensity, is accentuated in three dimensional flow to the extent that the prism is completely stable at 11% turbulence.

2.3. Non-Linear Aspects of Large Amplitude Galloping Oscillations.

The approach outlined in section 2.1 provides a means of assessing the susceptibility of prismatic bodies to the onset of high speed galloping. However, these oscillations do reach a maximum as indicated in Fig. 2.5, but the linear approach provides no information about limit cycles. In addition, information about hard oscillators is unavailable using linear theory. The required information, including the stability diagram, can either be obtained from experiments or non-linear approximations of the dynamical system.

The variety of galloping response is intrinsically linked to the shape of the transverse force characteristic, as illustrated in Fig. 2.6 (Novak, 1971). In this figure A_1 is $\left.\frac{dC_y}{d\alpha}\right|_{\alpha=0}$ and would be used to determine the critical speed, U_0 in this figure. Fig. 2.6(a) is typical of a 2/1 rectangle in slightly turbulent flow (see Fig. 2.4), and indicates that the amplitude of galloping oscillations continuously grows with wind speed above the critical value. Fig. 2.6(b) corresponds to the same geometry in smooth flow, from which it can be deduced that the oscillation amplitude grows from a non-zero value at speeds beyond the critical speed. As the wind speed is reduced, oscillations persist to speeds below the critical value, producing a hysteresis in the response predominantly due to the curvature of the transverse force. In addition, galloping could originate in this case at speeds below the critical speed if a sufficient initial disturbance is provided (above the dashed curve). Fig. 2.6(c) illustrates the hard oscillator characteristics of a 1/2 rectangle in smooth flow, as predicted from Fig 2.4(a). The response diagram again indicates the possibility of galloping oscillations at speeds greater than a critical value, corresponding to the magnitude of A_1, given a sufficient disturbance.

For all three cases the critical speed for the onset of galloping oscillations is directly proportional to structural damping. Indeed both rectangles are actually unstable as damping

approaches zero, as indicated by the asymptotes (dashed lines).

First attempts at modelling the non-linear effects due to large amplitude galloping oscillations were made by Parkinson and Brooks (1961). Developments of this and other methods were discussed by Parkinson (1974). The basic approach has been to expand the transverse force coefficent as a power series in $\tan\alpha$, or $\frac{\dot{y}}{V}$. A method which has gained substantial popularity utilises the idea of *universal response curves* (Novak, 1969; Novak, 1972; Novak and Tanaka, 1974). Novak (1969) suggested a seventh order polynomial in odd powers of $\frac{\dot{y}}{V}$ for a symmetric body, with an appropriately signed second order term to improve curve fitting ability:

$$C_{F_y} = A_1\left(\frac{\dot{y}}{V}\right) - A_2\left(\frac{\dot{y}}{V}\right)^2 \frac{\dot{y}}{|\dot{y}|} - A_3\left(\frac{\dot{y}}{V}\right)^3 + A_5\left(\frac{\dot{y}}{V}\right)^5 - A_7\left(\frac{\dot{y}}{V}\right)^7$$

where the A_i are coefficients of the curve fit to the static aerodynamic characteristic.

Substituting the above expression into the dynamical equation, and rearranging, the resulting non-linear differential equation is of the form:

$$m\ddot{y} + f(\dot{y})\dot{y} + k\,y = 0$$

which describes self-excited oscillations with finite amplitude. The function $f(\dot{y})$ is the total damping which includes the non-linear representation of the aerodynamic transverse force. The equation can be solved approximately by the method of slowly varying parameters (Minorsky, 1962). The solution is assumed to be of the form:

$$y = a\cos(\omega t + \phi)$$

where a and ϕ are the amplitude and phase which are assumed to vary only slightly over one cycle of vibration, and ω is the frequency of vibration (rad/sec). Hence the following equations can be deduced:

$$\dot{y} = -a\,\omega\sin(\omega t + \phi) \qquad \text{and} \qquad \dot{a}\cos(\omega t + \phi) - a\dot{\phi}\sin(\omega t + \phi) = 0$$

Expressions for the time varying amplitude and phase can be obtained by averaging over one cycle, after substituting the solution into the governing equation:

$$\dot{a} = \frac{1}{2\pi\omega m}\int_0^{2\pi} f(\dot{y})\sin\Phi\, d\Phi \qquad \text{and} \qquad \dot{\phi} = \frac{1}{2\pi\omega m a}\int_0^{2\pi} f(\dot{y})\cos\Phi\, d\Phi$$

The limit amplitude of steady vibrations, $\bar{a}$, is obtained by solving the polynomial resulting from the condition $\dot{a} = 0$. The solution in general can be written in the form:

$$\bar{a} = V_r f\left(A_i, \frac{V_r}{c_r}\right) \quad \text{or} \quad \frac{\bar{a}}{c_r} = \frac{V_r}{c_r} f\left(A_i, \frac{V_r}{c_r}\right)$$

where A_i, V_r and c_r are the aerodynamic coefficients, reduced velocity and reduced damping respectively. The form of the expression on the right has universal applicability to bodies of a particular section when provided as curves of $\bar{a}/c_r$ vs V_r/c_r. This means that a particular curve can be applied to a similar structure with different mass and damping properties oscillating in the same modes. Novak (1974) has extended the method to include oscillations in various modes with the effects of turbulence. Typical results are illustrated in Fig. 2.7, where the axis variables are constant factors of $\bar{a}/c_r$ and V_r/c_r.

2.4. Effect of Reduced Structural Damping.

The validity of the quasi-steady aerodynamic theory described in section 2.1 depends on a clear separation between the excitation due to vortex shedding and that due to galloping. As mentioned in section 2.1, a minimum factor of four should separate the predicted reduced velocities for the onset of galloping and vortex excitation. However, for low values of reduced damping the lower reduced velocities for onset of galloping correspond to flow regimes governed by unsteady aerodynamics. In particular, the presence of a non-linear wake and vortex shedding play an important role in the aerodynamic forcing. Furthermore, the boundaries between instabilities due to vortex excitation and galloping become blurred: the initiating mechanism is normally rooted in vortex shedding, but subsequently develops into a galloping instability.

This phenomenon is illustrated clearly in Fig. 2.8 (Novak, 1971). The critical reduced galloping speed predicted from the quasi-steady theory varies from 5.2 at 0.37% damping to 29.6 at 2.12% damping. However, galloping type oscillations grow from a reduced velocity of about 12, independent of structural damping over the above range. This corresponds to the critical Strouhal number for a 2/1 rectangle, which indicates that the instability is induced by vortex shedding but develops into a galloping mode. This pattern is not replicated, however, at 4.4% damping, where the rectangular prism exhibits a classic vortex shedding instability. The reason for this is clear, given that the corresponding reduced critical galloping speed is 61.5. The two modes of instability are thus well separated and the quasi-steady theory applies. The strong oscillations at the lowest damping levels around a reduced velocity of 5 correspond to a lock-in excitation due to a weak vortex forcing system. These oscillations vanish with small increases in damping.

2.5. Methods of Preventing Galloping Excitation.

The avoidance of high speed galloping oscillations can be approached from either, or both, a structural or aerodynamic perspective. The main aim of the prevention mechanisms is to ensure that the prismatic structure does not cross the stability boundary.

The structural means normally aim to raise the critical speed above that which would be expected to occur. From the critical velocity equation the mass, natural frequency and damping are the structural parameters which exert influence. Noting that $mN \propto \sqrt{km}$, increasing the mass or stiffness will raise the critical velocity, although this may not always be practical. Additional damping is a common means of suppressing many types of oscillatory behaviour, and the effect would be to raise the critical velocity for galloping. This approach is of particular benefit in cases of low reduced damping, where the aim is to prevent the growth of galloping oscillations by suppressing the initiating mechanism, vortex excitation.

The aerodynamic means of prevention are based on the desire to alter the flow structure so that the aerodynamic coefficients are stabilizing rather than destabilizing. The principal approach involves increasing the drag and/or eliminating the negative lift slope for the body. As for vortex excitation venting air through perforations has been shown to have a marked beneficial effect in certain cases (Whitbread *et al.*, 1970). The important features of the aerodynamic mechanism are:

(a) reducing the distance between the separating streamlines and the sides of the prism afterbody;

(b) generating transverse forces counteracting the exciting forces.

Studies have been carried out on the effect of attaching fins to prisms, or, alternatively, making corner cuts (Naudascher *et al.*, 1981; Shiraishi *et al.*, 1988). Properly designed fins can be shown to produce both effects (a) and (b) , as illustated in Fig. 2.9: fins located near the front stagnation zone have a streamlining effect, and those on the sides generate damping forces. Various configurations were presented by Naudascher *et al.* (1981), who performed a series of tests on modified square prisms, Fig. 2.10. A summary of the results obtained are illustrated in Fig. 2.11. The configurations (a), (c) and (e) in Fig. 2.10 all exhibit stable configurations about the zero incidence position, with (a) stable at all incidences tested. The other configuratons show a reduction in either the negative slope of the transverse force or the range over which the slope is negative, compared with the reference square. Naudascher reported that for arrangements (c), (e) and (f) in Fig. 2.10, two states of quasi-steady flow were observed, characterized by pairs of distinct lift and drag coefficients. Shiraishi *et al.* (1988) tested a corner-cut rectangular prism of aspect ratio 1.46. Although the test results on the sectional model were encouraging, insofar as an optimum configuration was determined, Fig. 2.12, results on a full scale model of the rectangular section pylon members of a cabled-stayed bridge were inconclusive.

3. APPLICATION TO THE EXTERNAL FRAME OF THE TOWER HOTEL.

The information on the external frame of the Tower Hotel, which forms the basis of the stability considerations herein, has been obtained from the report of the wind tunnel tests carried out by BMT Fluid Mechanics Ltd. (Coleman and Davies, 1994). Additional information on mode shapes, periods, mass and damping has been supplied by Prof. N.D.P. Barltrop of the Department of Naval Architecture and Ocean Engineering at the University of Glasgow, on behalf of W.S. Atkins and Partners Overseas.

3.1. External Frame Arrangement.

The numbering system used to identify the external frame components is illustrated in Fig. 3.1. Of primary concern is the susceptibility to galloping excitation of members 1 to 4. Components 5 to 7 are lattice frameworks which are not particularly prone to this form of instability. Members 8 to 10 present a low aspect ratio cross-section to a horizontal wind. The cross-wind direction for these members, therefore, corresponds to the greater rigidity and hence higher natural frequency. Combined with the fact that the oscillator characteristics of low aspect ratio sections are hard in smooth flow (see section 2.2), and weakly soft in turbulent flow (Fig. 2.4), the likelihood of cross-wind oscillations due to high speed galloping is remote.

Extending from the top of the Tower Hotel by a height of 57m is a slender mast (Fig. 1.1), which tapers to a circular cross-section at the top. The base section of the mast has the cross-section illustrated in Fig. 3.2. No literature has been found against which the stability of the mast can be assessed. However, the slenderness, shape, cantilevered root fixing and exposure to higher wind speeds of low turbulence intensities mean that galloping could possibly occur. It is recommended that an investigation of the aeroelastic stability of the mast be carried out, the expertise being available within the Department of Aerospace Engineering at the University of Glasgow.

3.2. Wind Speed and Relevant Frame Design Data.

The design mean hourly wind speeds, on which the cross-wind stability of frame members 1 to 4 is based, are given in Table 1. Also given in this table are the relevant mass and geometric properties of the members. Consultants at W.S. Atkins have performed a dynamic finite element analysis of the external frame from which a set of natural frequencies and mode shapes have been obtained. The data from the first twenty modes are given in Table 2. Selected mode shapes, corresponding to the lowest frequencies at which each of members 1 to 4 are apparently excited, are illustrated in Fig. 3.3.

The local wind conditions at the location of the frame members for a range of wind directions was investigated by BMT. Results from tests on the model hotel are presented in Table 3.

The reference speed corresponds to the mean wind speed at a height of 214.4m above the ground (roof level), and the sign convention used for wind direction is illustrated in Fig. 3.4. For mean wind directions between 270° and 345° the turbulence intensities are decreasing, and local wind speeds increasing, at the member locations. This is due to the gradual emergence of the members from the interference effects from the windward side of the hotel. Between 345° and 30° the local wind speeds are greater than the reference value, due to the acceleration of the flow as it diverts around the sides. This is accompanied by turbulence intensities close to reference values, although these increase to a maximum at 210°. This latter change is probably due to vortical flow structures originating from the lift shaft.

3.3. Stability of External Frame Members.

An assessment of the wind speed above which galloping oscillations are likely to grow can be made based on the linear theory outlined in section 2.1. However, it must be stressed that this theory is based on isolated two dimensional flow conditions, which will only be approximated around the external frame of the Tower Hotel. Notwithstanding these limitations, a lower bound critical wind speed can be calculated, provided the damping ratios preclude a coupling with vortex excitation.

To ensure validity of the galloping theory, the minimum damping ratios required should correspond to a critical reduced velocity of about 50 ($4/S_{crit}$, $S_{crit} = 0.08$ for a 2/1 rectangle). The actual velocity for onset of galloping can then be calculated and compared with the design speed. The likelihood of achieving the required damping ratios can also be addressed. In addition, values of mass, natural frequency and transverse force coefficient derivative are required to perform the calculation. The minimum turbulence intensity on any member is 9.3%, which occurs at mean wind directions of 45° and 122.5° (Table 3). From Table 1 the aspect ratio of all members is close to 2/1, hence the data for a 2/1 rectangle in Fig. 2.4(b) provides an approximate slope of the force coefficient :

$$\left.\frac{dC_y}{d\alpha}\right|_{\alpha=0} \approx 1.4 \quad \text{for 9\% turbulence}$$

Table 4 presents the results of the calculations for members 1 to 4, giving the minimum damping ratios required and the corresponding critical galloping speeds. These damping ratios are conservative insofar as the increasing turbulence intensity in the lower bays would reduce the transverse force derivative, and hence reduce the minimum damping. In addition, the actual wind speeds normal to the cross-sections of the members in the upper bays would be less than the design speeds due to curvature of the frame. The natural frequencies correspond to the modes indicated in Fig. 3.3, and an air density of $1.2\,kg/m^3$ has been assumed. From Table 4 it is evident that the predicted critical galloping speeds are well in excess of the design speeds.

Based on the data in Blevins (1990), steel towers have a minimum damping ratio of about 0.16%, with 90% of towers having a damping ratio above 0.32%. These values include foundation damping, the lowest values corresponding to rock foundations. Assuming that a value of 0.16% is a reasonable lower limit, the upper bays require dampers. However, the actual damping in the lowers bays may be raised by the foundations and the effect of the added dampers in the upper bays. The required damping may be achievable without added dampers in the lower bays.

4. CONCLUSIONS.

From the survey of high speed galloping excitation of rectangular prisms presented in this report, with particular reference to the Tower Hotel of the Chicago Beach Development, a number of conclusions can be drawn, and these are listed below.

- The tendency of prismatic bodies to develop high speed transverse galloping oscillations can be assessed effectively by employing quasi-steady sectional aerodynamic theory, provided the reduced velocity is greater than that for vortex excitation by a factor of at least four, and the flow regime is approximately two-dimensional.

- Notwithstanding the above limitations, a necessary condition for the initiation of galloping oscillations from rest is the presence of a negative lift slope. Oscillations are predicted to occur at all wind speeds above a critical threshold.

- Aspect ratio (d/h) and freestream turbulence have a significant effect on the galloping tendency of a rectangular prism. In smooth flow, galloping is predicted to occur above a critical wind speed for $0.75 < d/h < 3$. However, the minimum aspect ratio reduces with increasing freestream turbulence. Below the lower threshold, galloping can only occur above a critical wind speed if a sufficient initial disturbance is supplied.

- Galloping oscillations, once initiated, will grow until a limit amplitude is reached. This post initiation behaviour can either be assessed by wind tunnel experiments or the use of non-linear representations of the quasi-steady transverse aerodynamic force. The stability characteristics of prismatic bodies are intrinsically linked to the shape of the transverse force curve.

- The characteristics of prism galloping are affected significantly by reduced damping. At low damping galloping is coupled with vortex excitation and the critical velocity is independent of damping ratio. In this region quasi-steady theory is invalid.

- Increasing the mass, stiffness, or damping of a prismatic structure will raise the critical

wind speed for the onset of galloping excitation. The aerodynamic means of prevention usually entail surface porosity, corner cuts or the attachment of suitably arranged fins to modify the streamline pattern and counteract the exciting forces.

- Based on the two-dimensional quasi-steady aerodynamic theory and supplied data, an assessment of the transverse galloping stability of the Tower Hotel exoskeleton has been made. At damping levels which enable a quasi-steady analysis to be carried out, the critical speeds are substantially in excess of those likely to occur. Hence the prospect of high speed transverse galloping is very remote.

- The added dampers, originally designed to suppress vortex excitation, play an important role in the suppression of galloping excitation in the upper two bays of the exoskeleton. The level of damping required in the lower two bays may be achievable without added dampers, depending on the level of foundation damping and the effect of the dampers in the upper bays.

- The aeroelastic stability of the mast which extends from the top of the Tower Hotel should be investigated. The unusual cross-section, from an aerodynamic perspective, means that a wind tunnel investigation would most probably be required.

REFERENCES.

Bearman, P.W.; Trueman, D.M.	1971	*An Investigation of the Flow around Rectangular Cylinders.* Imperial College Aero Report 71-15.
Blevins, R.D.	1990	*Flow-Induced Vibration.* Van Nostrand Reinhold, 2nd ed., p. 326
Brooks, N.P.H.	1960	*Experimental Investigation of the Aeroelastic Instability of Bluff Two-Dimensional Cylinders.* M.A.Sc. Thesis, Univ. British Columbia.
Coleman, S.A.; Davies, M.E.	1994	*Chicago Beach Resort Development - Wind Tunnel Tests.* BMT Report, Project No. 43049.
Den Hartog, J.P.	1930	*Transmission Line Vibration due to Sleet.* Trans. A.I.E.E., vol. 49, p. 444.
Laneville, A.; Parkinson, G.V.	1971	*Effects of Turbulence on Galloping of Bluff Cylinders.* Proc. 3rd Intern. Conf. on Wind Effects on Buildings and Stuctures, Tokyo, p. 787-797.
Minorsky, N.	1962	*Non-Linear Oscillations.* D. Van Nostrand and Co., New York.
Nakamura, Y.	1990	*Recent Research into Bluff-Body Flutter.* J. Wind Engineering and Industrial Aerodynamics, vol. 33, p. 1-10.
Nakamura, Y.	1993	*Bluff-Body Aerodynamics and Turbulence.* J. Wind Engineering and Industrial Aerodynamics, vol. 49, p. 65-78.
Nakamura,Y.; Hirata,K.	1993	*The Aerodynamic Mechanism of Galloping.* Trans. Japan Soc. Aero. Space Sci., vol. 36, No. 114, p. 257-269.
Naudascher, E.; Weske, J.R.; Fey, B.	1981	*Exploratory Study on Damping of Galloping Vibrations.* J. Wind Engineering and Industrial Aerodynamics, vol. 8, p. 211-222.
Novak, M.	1969	*Aeroelastic Galloping of Prismatic Bodies.* Proc. A.S.C.E., J. Eng. Mech. Div., vol. 95, EM1, p. 115-142.
Novak, M.	1971	*Galloping and Vortex Induced Oscillations of Structures.* Proc. 3rd Intern. Conf. on Wind Effects on Buildings And Stuctures, Tokyo, p. 799-809.
Novak, M.	1972	*Galloping Oscillations of Prismatic Structures.* Proc. A.S.C.E., J. Eng. Mech. Div., vol. 98, No. 1, EM1, p. 27-46.
Novak, M.; Tanaka, H.	1974	*Effect of Turbulence on Galloping Instability.* Proc. A.S.C.E., J. Eng. Mech. Div., vol. 100, EM1, p. 27-47.
Parkinson, G.V.; Brooks, N.P.H.	1961	*On the Aeroelastic Instability of Bluff Cylinders.* Trans. A.S.M.E., J. Appl. Mech, vol. 28, p. 252-258.
Parkinson, G.V.	1974	*Mathematical Models of Flow-Induced Vibrations of Bluff Bodies.* Flow-Induced Structural Vibrations, ed. Naudascher, E., Springer-Verlag, p. 81-127.

Shiraishi, N.; Matsumoto, M.; Shirato, H.; Ishizaki, H. 1988 *On Aerodynamic Stability Effects for Bluff Rectangular Cylinders by their Corner-Cut.* J. Wind Engineering and Industrial Aerodynamics, vol. 28, p. 371-380.

Smith, J.D. 1962 *An Experimental Study of the Aeroelastic Instability of Rectangular Cylinders.* M.A.Sc. Thesis, Univ. British Columbia.

Whitbread, R.E.; Cowdrey, C.F.; O'Neill, P.G. 1970 *A Wind-Tunnel Investigation for the Proposed British Pavillion for Expo 70, Alaska, Japan.* NPL/Aero Special Report No. 037, Teddington.

Table 1. Properties of External Frame Members.

Frame Mid-Height (m)	Wind Speed (m/s)	Cross-Section Dimensions (m)	Aspect Ratio	Mass per Unit Length (kg/m)	Length (m)
238	50.8	5.6 × 3	1.87	2360	96
164	50.3	6.4 × 3	2.13	3150	65.6
100	46.9	6.5 × 3	2.17	4360	62.8
38	43.0	6.5 × 3	2.17	5560	62

Table 2. Summary of Modal Data for External Frame.

MODE NUMBER	EIGENVALUE	ANGULAR FREQ.	PERIOD (s)	FREQUENCY (Hz)
1	2.1056E+01	4.5886E+00	1.3693E+00	7.3031E-01
2	3.2432E+01	5.6949E+00	1.1033E+00	9.0637E-01
3	3.3984E+01	5.8296E+00	1.0778E+00	9.2781E-01
4	5.2545E+01	7.2488E+00	8.6679E-01	1.1537E+00
5	9.3919E+01	9.6912E+00	6.4834E-01	1.5424E+00
6	1.0000E+02	1.0000E+01	6.2831E-01	1.5916E+00
7	1.1551E+02	1.0748E+01	5.8461E-01	1.7106E+00
8	1.1574E+02	1.0758E+01	5.8404E-01	1.7122E+00
9	1.2396E+02	1.1134E+01	5.6434E-01	1.7720E+00
10	1.2397E+02	1.1134E+01	5.6431E-01	1.7721E+00
11	1.2592E+02	1.1221E+01	5.5993E-01	1.7859E+00
12	1.2598E+02	1.1224E+01	5.5980E-01	1.7864E+00
13	1.3476E+02	1.1609E+01	5.4124E-01	1.8476E+00
14	1.3673E+02	1.1693E+01	5.3734E-01	1.8610E+00
15	1.3791E+02	1.1743E+01	5.3504E-01	1.8690E+00
16	1.3840E+02	1.1764E+01	5.3409E-01	1.8723E+00
17	1.4043E+02	1.1850E+01	5.3021E-01	1.8861E+00
18	1.4044E+02	1.1851E+01	5.3020E-01	1.8861E+00
19	1.6518E+02	1.2852E+01	4.8888E-01	2.0455E+00
20	1.6916E+02	1.3006E+01	4.8309E-01	2.0700E+00

Table 3. Wind Speed, Direction And Turbulence Intensity at Selected Frame Locations.

Wind Direction	Measured Quantity	Frame Location			
		1	2	3	4
270°	V/Vref	1.12	0.40	0.37	0.31
	Local Wind Direction (degs)	265	268	269	268
	Turbulence Intensity (%)	24.7	42.9	48.7	49.7
285°	V/Vref	1.17	0.39	0.35	0.35
	Local Wind Direction (degs)	286	286	282	282
	Turbulence Intensity (%)	16.2	38.7	45.2	51.5
300°	V/Vref	1.16	0.44	0.46	0.56
	Local Wind Direction (degs)	293	299	301	299
	Turbulence Intensity (%)	10.8	37.9	37.7	33.9
315°	V/Vref	1.14	0.62	0.86	0.88
	Local Wind Direction (degs)	311	312	307	306
	Turbulence Intensity (%)	10.2	30.9	25.1	21.6
330°	V/Vref	1.07	0.69	0.97	0.94
	Local Wind Direction (degs)	331	322	319	321
	Turbulence Intensity (%)	12.0	29.5	19.7	22.5
345°	V/Vref	1.13	1.12	1.07	1.04
	Local Wind Direction (degs)	334	313	311	312
	Turbulence Intensity (%)	12.9	12.7	12.7	14.1
0°	V/Vref	1.14	1.13	1.06	1.04
	Local Wind Direction (degs)	344	325	324	323
	Turbulence Intensity (%)	11.3	12.0	12.0	13.0
15°	V/Vref	1.11	1.13	1.05	1.01
	Local Wind Direction (degs)	10	354	353	352
	Turbulence Intensity (%)	10.1	11.2	11.9	13.7
30°	V/Vref	1.05	1.09	1.03	0.98
	Local Wind Direction (degs)	24	9	8	8
	Turbulence Intensity (%)	9.7	11.3	12.2	13.1
45°	V/Vref	0.98	0.85	0.79	0.73
	Local Wind Direction (degs)	42	27	28	27
	Turbulence Intensity (%)	9.3	15.9	18.1	20.3
122.5°	V/Vref	1.06	0.72	0.72	0.76
	Wind Direction (degs)	128	146	144	137
	Turbulence Intensity (%)	9.3	14.2	15.7	18.8
195°	V/Vref	1.17	1.16	1.08	0.99
	Local Wind Direction (degs)	195	198	199	198
	Turbulence Intensity (%)	17.3	11.6	13.1	16.7
210°	V/Vref	0.70	0.82	0.68	0.58
	Local Wind Direction (degs)	212	205	206	206
	Turbulence Intensity (%)	37.0	41.4	47.7	51.4

Table 4. Minimum Damping Ratios and Critical Galloping Speeds for External Frame Members 1 to 4.

Member No.	Mass per Unit Length (kg/m)	Natural Frequency (Hz)	Minimum Damping Ratio for $V_r = 50$ (%)	Critical Galloping Speed (m/s)	Design Wind Speed (m/s)
1	2360	0.906	1.27	135.9	50.8
2	3150	1.154	0.95	173.1	50.3
3	4360	1.592	0.69	238.8	46.9
4	5560	1.786	0.54	267.9	43.0

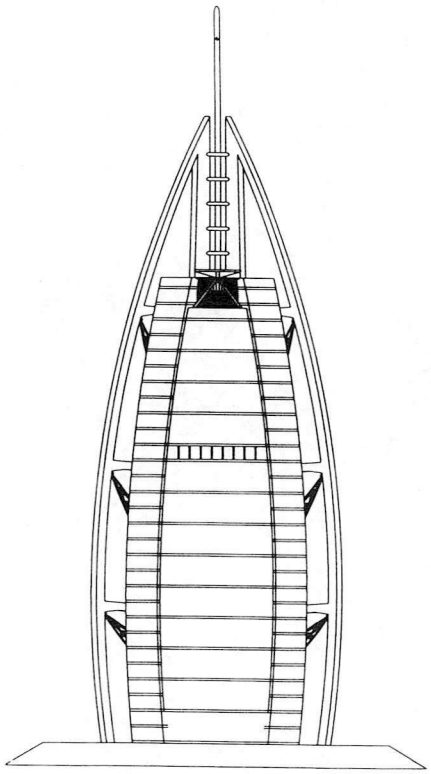

(a) Rear Elevation

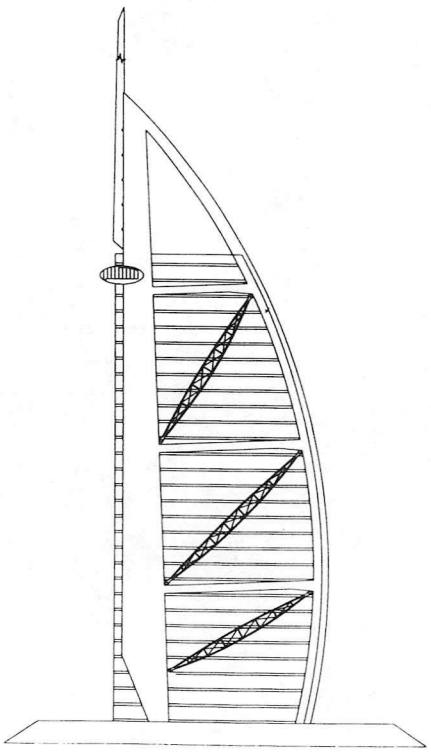

(b) Side Elevation

Fig. 1.1. Diagram of Tower Hotel.

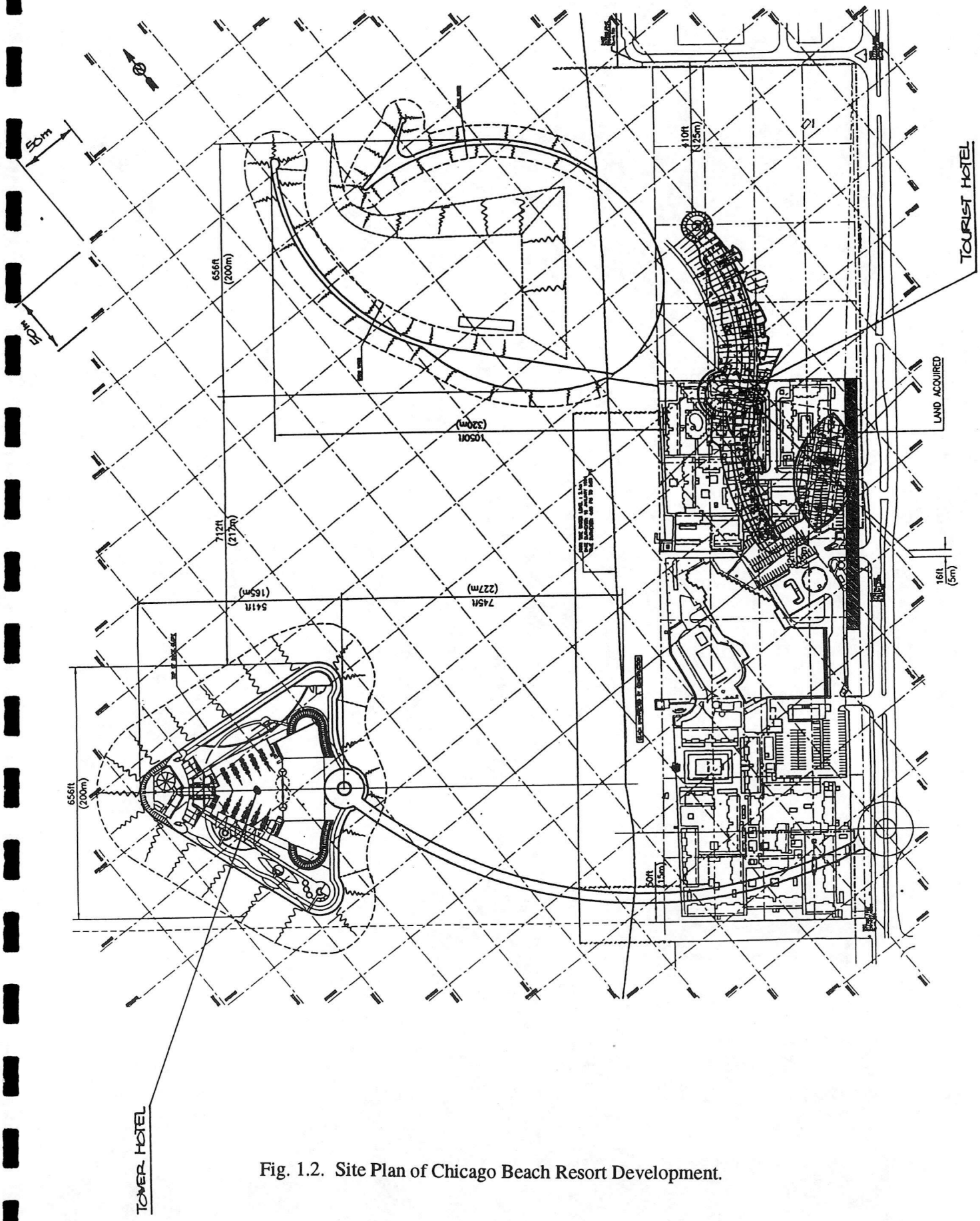

Fig. 1.2. Site Plan of Chicago Beach Resort Development.

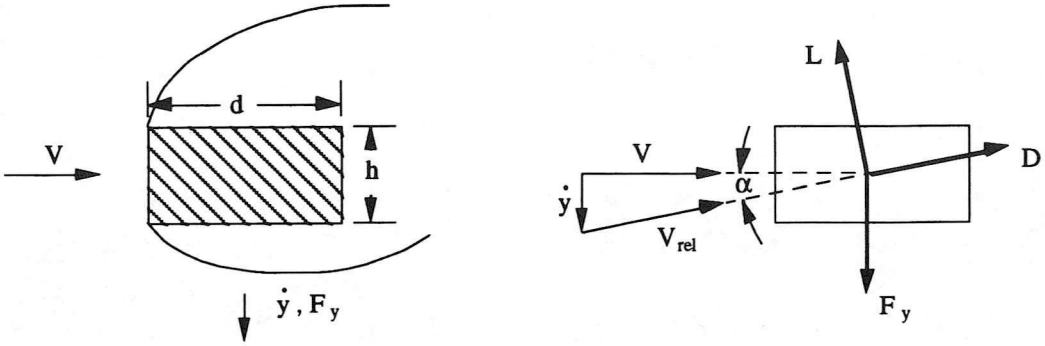

Fig. 2.1. Instantaneous Velocities and Forces on a Galloping Prism.

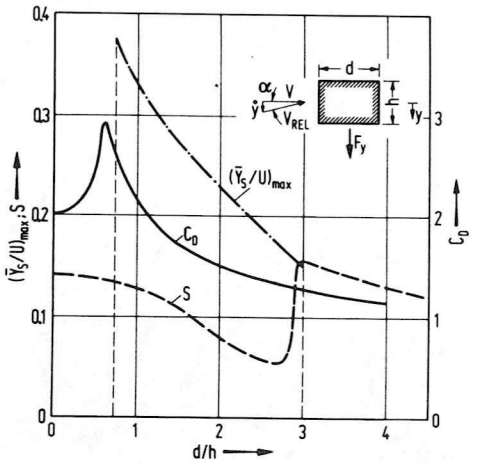

Fig. 2.2. Effect of Aspect Ratio on Galloping Response.

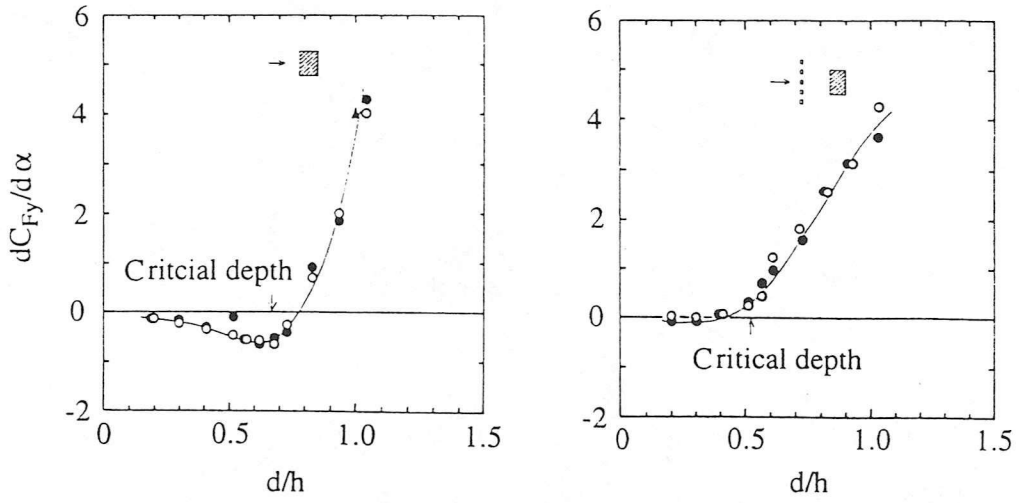

(a) Smooth Flow

(b) Turbulent Flow (12%)

Fig. 2.3. Effect of Aspect Ratio on Aerodynamic Transverse Force Derivatives.

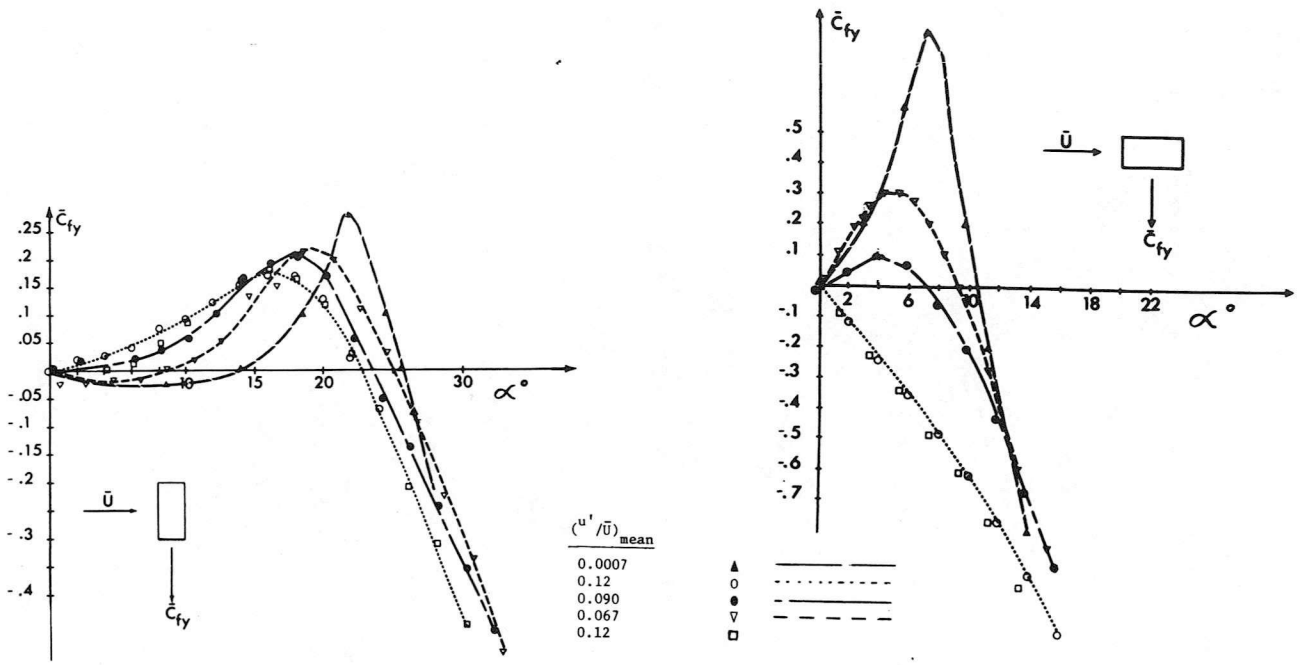

(a) $d/h = 0.5$

(b) $d/h = 2$

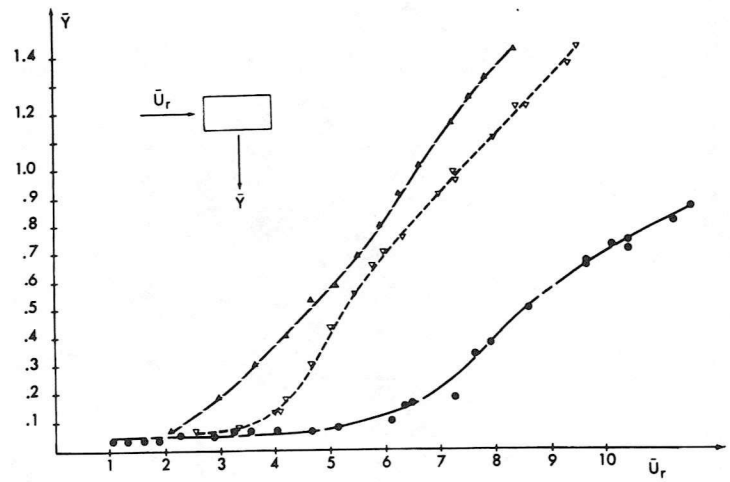

(c) Amplitude versus Reduced Velocity for 2/1 Rectangular Prism.

Fig. 2.4. Transverse Forces and Galloping Response Obtained from Tests on Rectangular Prisms.

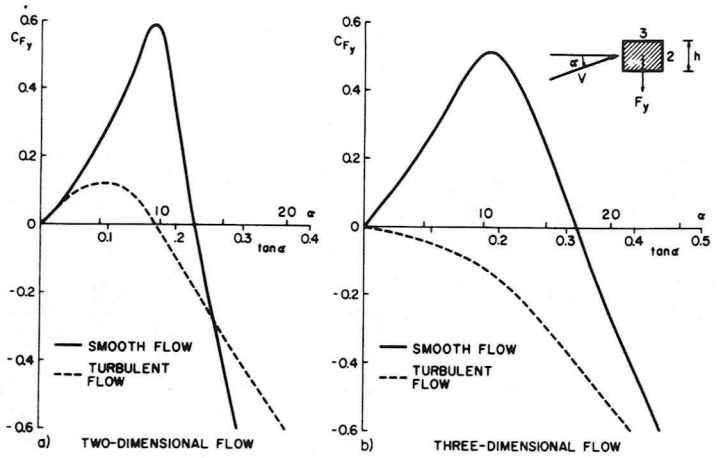

Fig. 2.5. Transverse Forces on a 3/2 Rectangular Prism in Smooth and Turbulent Flow.

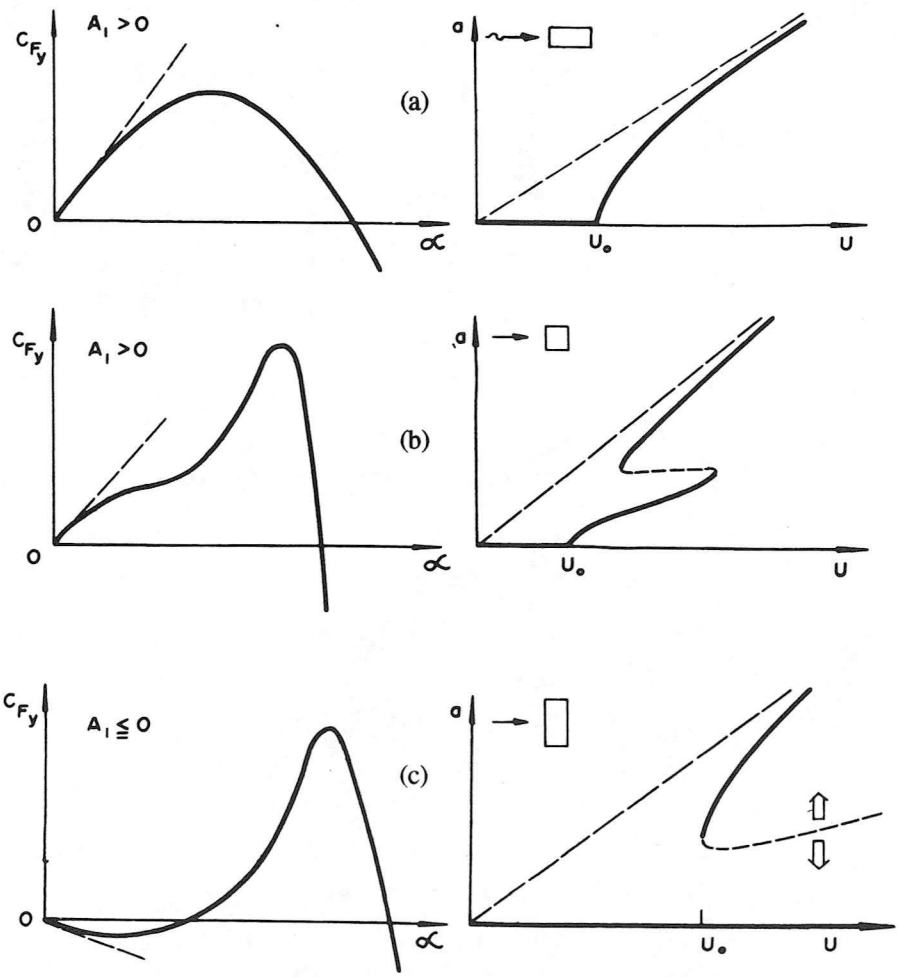

Fig. 2.6. Typical Transverse Forces with Associated Galloping Response.

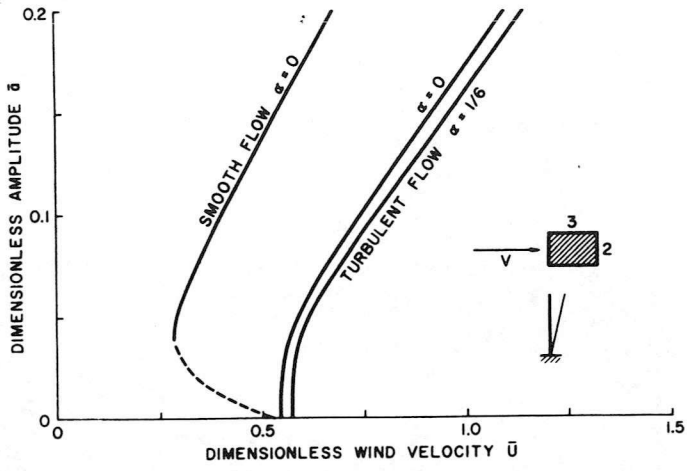

Fig. 2.7. Universal Galloping Response of a Cantilevered 3/2 Prism in Smooth and Turbulent (11%) Flow.

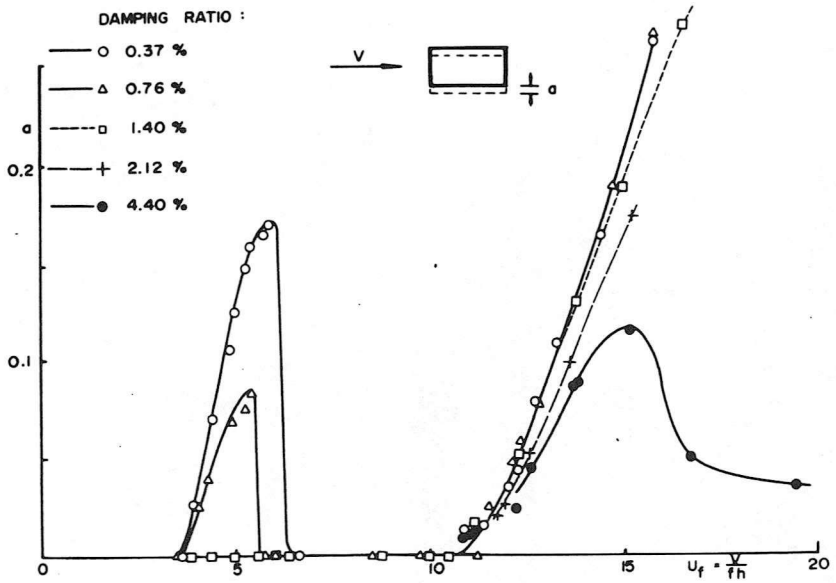

Fig. 2.8. Lateral Response of a Tall Building Model of 2/1 Rectangular Section.

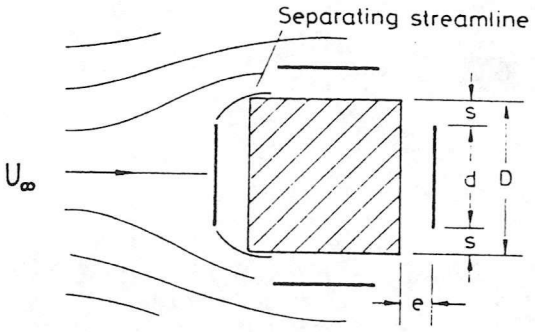

Fig. 2.9. Illustration of the Two Principles of Aerodynamic Damping Employed for the Suppression of Galloping.

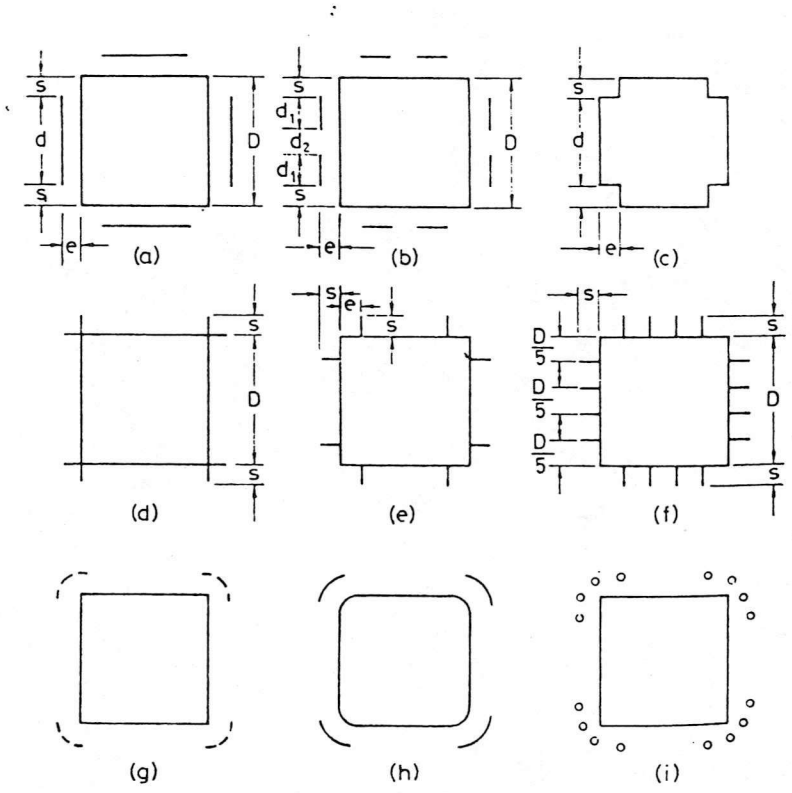

Fig. 2.10. Cross-Sectional Form of Prisms which Reduce Aerodynamic Instability.

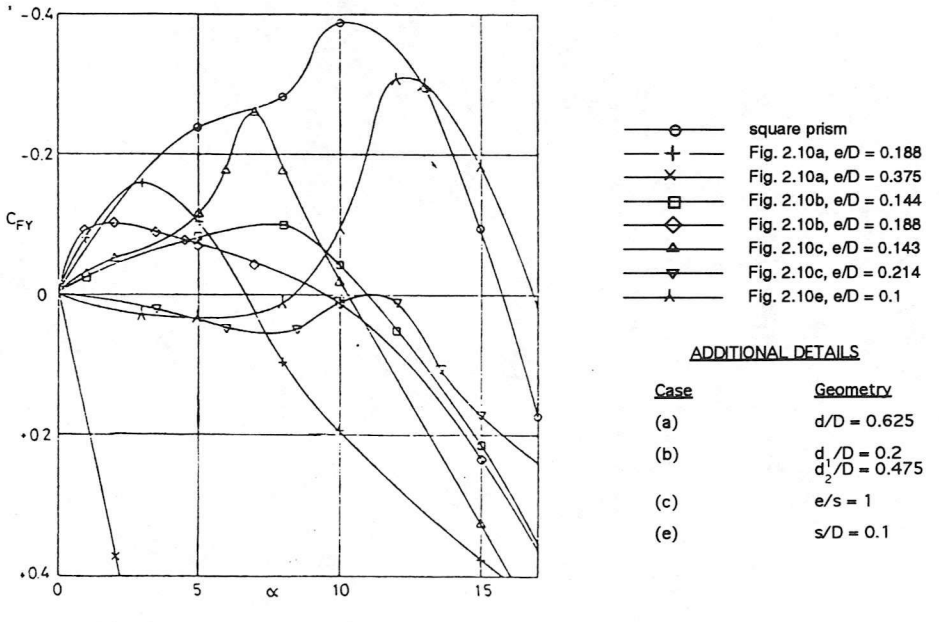

Fig. 2.11. Transverse Force Coefficient C_y for Various Damper Configurations.

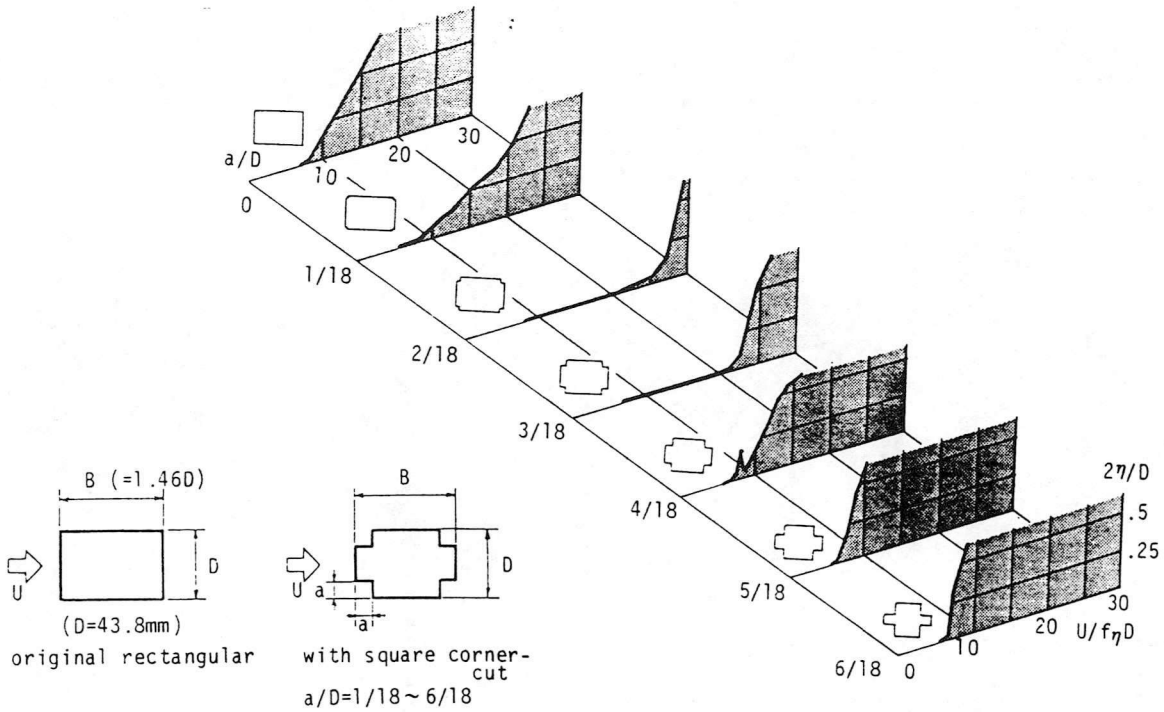

Fig. 2.12. Effect of Corner-Cut Size on Galloping Response of Rectangular Prisms.

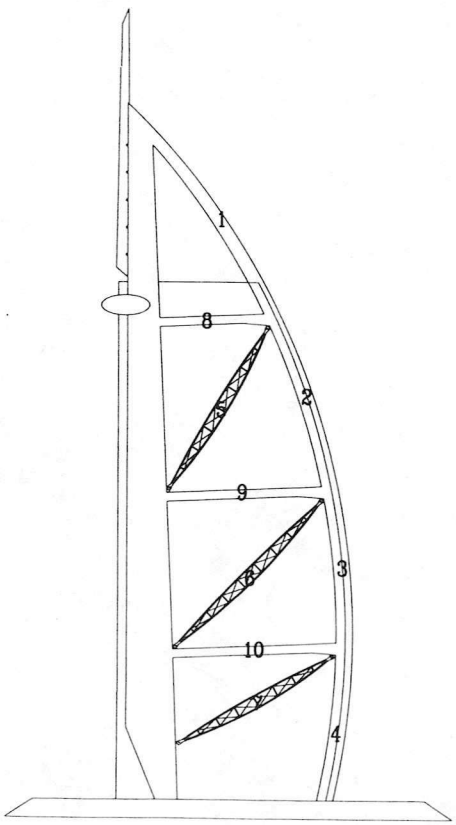

Fig. 3.1. Numbering System for External Frame Members.

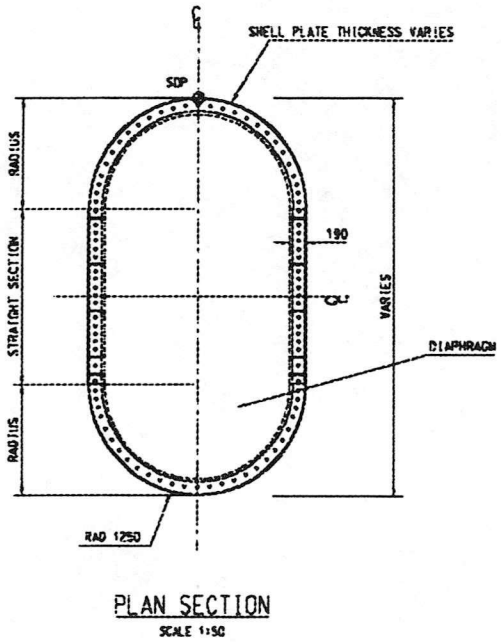

Fig. 3.2. Base Section of Tower Hotel Mast.

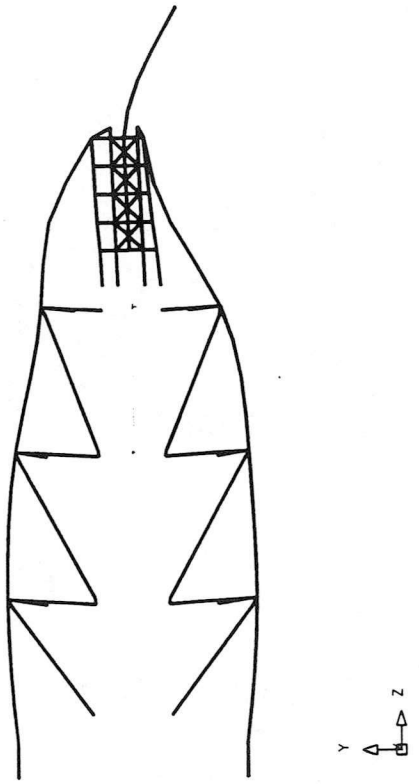

Member 1 - Mode 2

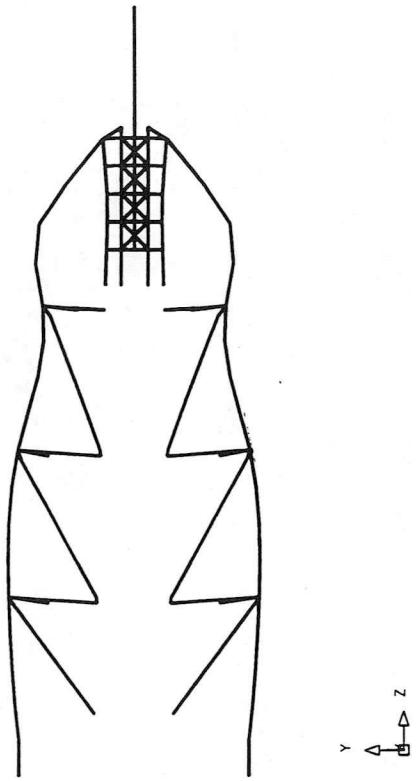

Member 2 - Mode 4

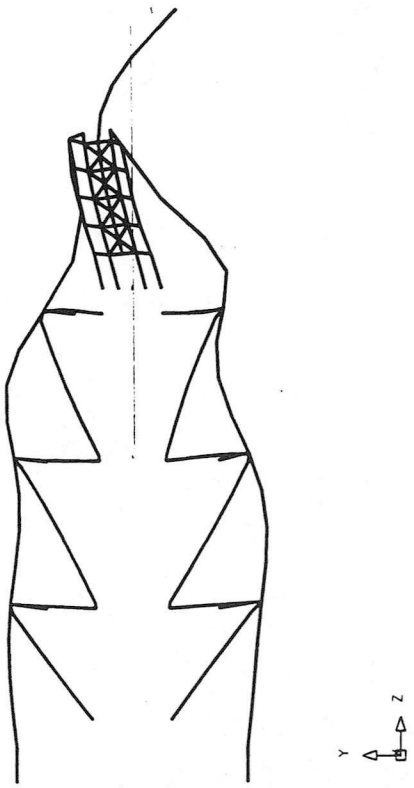

Member 3 - Mode 6

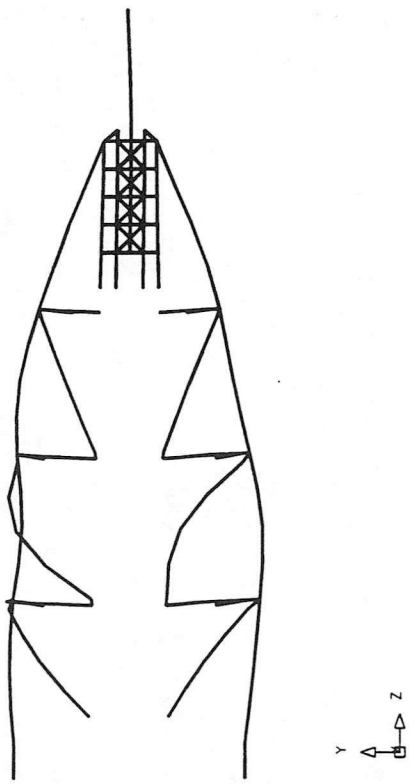

Member 4 - Mode 11

Fig. 3.3. Lowest Modes at which Frame Members are Apparently Excited.

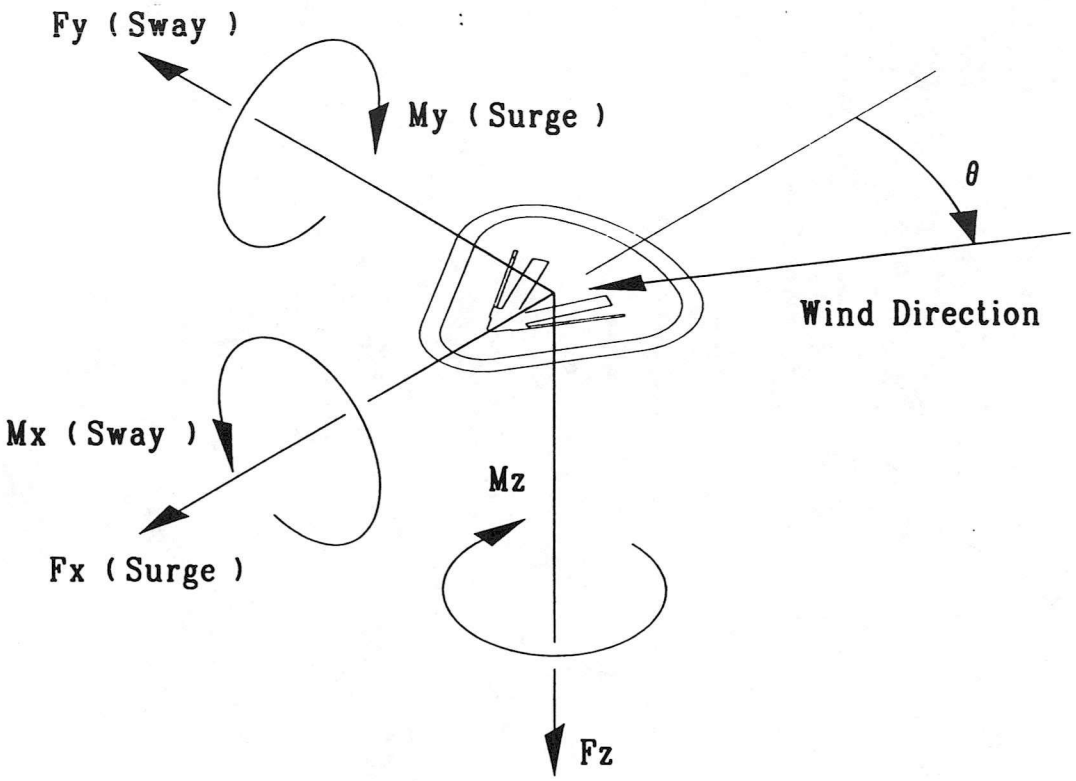

Fig. 3.4. Sign Convention for Wind Direction.